Detection of DNA Hybridization on Gold Surfaces by Polarization Modulation Infrared Reflection Absorption Spectroscopy

ARTICLE *in* LANGMUIR · MAY 2002

Impact Factor: 4.46 · DOI: 10.1021/la025613z

5 AUTHORS, INCLUDING:

Simon E Lappi
North Carolina State University
45 PUBLICATIONS **1,567** CITATIONS

Detection of DNA Hybridization on Gold Surfaces by Polarization Modulation Infrared Reflection Absorption Spectroscopy

Scott H. Brewer,[†] Selina J. Anthireya,[†] Simon E. Lappi,[†] David L. Drapcho,[‡] and Stefan Franzen*,[†]

Department of Chemistry, North Carolina State University, Raleigh, North Carolina 27695, and Digilab Division, Bio-Rad Laboratories, 68 Mazzeo Drive, Randolph, Massachusetts 02368

Received February 7, 2002. In Final Form: February 12, 2002

Polarization modulation infrared reflection absorption spectroscopy (PM-IRRAS) was used to detect DNA hybridization on gold surfaces. Mixed monolayers of 6-mercapto-1-hexanol (MCH) and single-stranded DNA (ssDNA) with a C6−SH 5′ modifier were first formed on the gold surface by co-deposition. Then hybridization with the complementary ssDNA strand was performed to obtain double-stranded DNA (dsDNA). The PM-IRRAS spectra obtained contained absorptive features indicative of DNA arising from the phosphodiester backbone and the purine and pyrimidine rings. An infrared signature of dsDNA was observed at 1655 cm^{-1} that was absent in the ssDNA spectra. This band permitted the distinction between ssDNA and dsDNA to be made thus allowing for the detection of DNA hybridization on gold surfaces by PM-IRRAS.

Introduction

The detection of DNA hybridization on surfaces is an area of intense current investigation. A number of methods have recently been employed for analysis of surface hybridization including fluorescence,[1−4] chronocoulometry,[5−7] surface plasmon resonance,[8,9] and colloidal labeling of nanoparticles.[10−12] The hybridization of DNA on gold surfaces is of particular interest because of the wide use of self-assembled monolayers on gold. However, despite the well-developed application of grazing angle Fourier transform infrared spectroscopy[13,14] there has been no direct detection of DNA hybridization on self-assembled monolayers of DNA. There have been numerous experimental studies on the DNA bases by infrared spectroscopy[15−25] and nonresonant[16,21,25−31] and resonant Raman spectroscopy.[32−36] These studies include using vibrational spectroscopy to probe B, A, and Z DNA forms[37−42] and to study drug and protein binding to DNA.[43−46] The vibra-

* To whom correspondence should be addressed. Phone: (919)-515−8915. Fax: (919)-515-8909. E-mail: Stefan_Franzen@ncsu.edu.
† North Carolina State University.
‡ Bio-Rad Laboratories.

(1) Fodor, S. P. A.; Read, J. L.; Pirrung, M. C.; Stryer, L.; Lu, A. T.; Solas, D. *Science* **1991**, *251*, 767−773.
(2) Lockhart, D. J.; Winzeler, E. A. *Nature* **2000**, *405*, 827−836.
(3) Bulyk, M. L.; Gentalen, E.; Lockhart, D. J.; Church, G. M. *Nat. Biotechnol.* **1999**, *17*, 573−577.
(4) Chee, M.; Yang, R.; Hubbell, E.; Berno, A.; Huang, X. C.; Stern, D.; Winkler, J.; Lockhart, D. J.; Morris, M. S.; Fodor, S. P. A. *Science* **1996**, *274*, 610−614.
(5) Esch, M. B.; Locascio, L. E.; Tarlov, M. J.; Durst, R. A. *Anal. Chem.* **2001**, *73*, 2952−2958.
(6) Steel, A. B.; Herne, T. M.; Tarlov, M. J. *Anal. Chem.* **1998**, *70*, 4670−4677.
(7) Steel, A. B.; Herne, T. M.; Tarlov, M. J. *Bioconjugate Chem.* **1999**, *10*, 419−423.
(8) He, L.; Musick, M. D.; Nicewarner, S. R.; Salinas, F. G.; Benkovic, S. J.; Natan, M. J.; Keating, C. D. *J. Am. Chem. Soc.* **2000**, *122*, 9071−9077.
(9) Brockman, J. M.; Frutos, A. G.; Corn, R. M. *J. Am. Chem. Soc.* **1999**, *121*, 8044−8051.
(10) Sauthier, M.; Carroll, R.; Gorman, C.; Franzen, S. *Langmuir* **2002**, *18*, 1825−1830.
(11) Cao, Y. W.; Jin, R.; Mirkin, C. A. *J. Am. Chem. Soc.* **2001**, *123*, 7961−7962.
(12) Demers, L. M.; Mirkin, C. A.; Mucic, R. C.; Reynolds, R. A.; Letsinger, R. L.; Elghanian, R.; Viswanadham, G. *Anal. Chem.* **2000**, *72*, 5535−5541.
(13) Allara, D.; Nuzzo, R. *Langmuir* **1985**, *1*, 52−66.
(14) Allara, D.; Nuzzo, R. *Langmuir* **1985**, *1*, 45−52.
(15) Chin, S.; Scott, I.; Szczepaniak, K.; Person, W. B. *J. Am. Chem. Soc.* **1984**, *106*, 3415−3422.
(16) Delabar, J. M.; Majoube, M. *Spectrochim. Acta* **1978**, *34A*, 129−140.
(17) Falk, M.; Hartman, K. A.; Lord, R. C. *J. Am. Chem. Soc.* **1963**, *85*, 387−391.
(18) Graindourze, M.; Smets, J.; Zeegers-Huyskens, T. H.; Maes, G. *J. Mol. Struct.* **1990**, *222*, 345−364.
(19) Hirakawa, A. Y.; Okada, H.; Sasagawa, S.; Tsuboi, M. *Spectrochim. Acta* **1985**, *41A*, 209−216.
(20) Kyogoku, A. Y.; Higuchi, S.; Tsuboi, M. *Spectrochim. Acta* **1967**, *23A*, 969.
(21) Lewis, T. P.; Miles, H. T.; Becker, E. D. *J. Phys. Chem.* **1984**, *88*, 3253−3260.
(22) Thijs, R.; Zeeger-Huyskens, T. *Spectrochim. Acta* **1984**, *40A*, 307−313.
(23) Thomas, G. J., Jr. *Biopolymers* **1969**, *7*, 325−334.
(24) Tsuboi, M.; Kyogoku, Y.; Shimanouchi, T. *Biochim. Biophys. Acta* **1962**, *55*, 1−12.
(25) Tsuboi, M.; Takahashi, S.; Harada, I. *Infrared and Raman spectra of nucleic acids − Vibrations in the base residues*; Tsuboi, M., Takahashi, S., Harada, I., Eds.; Academic Press: London, 1973; Vol. 2, pp 92−143.
(26) Lane, M. J.; Thomas, G. J., Jr. *Biochemistry* **1979**, *18*, 3839−3846.
(27) Lord, R. C.; Thomas, G. J., Jr. *Spectrochim. Acta* **1967**, *23A*, 2551−2591.
(28) Lord, R. C.; Thomas, G. J., Jr. *Biochim. Biophys. Acta* **1967**, *142*, 1−11.
(29) Nishimura, Y.; Tsuboi, M.; Nakano, T.; Higuchi, S.; Sato, T.; Shida, T.; Uesugi, S.; Ohtsuka, E.; Ikehara, M. *Nucl. Acids Res.* **1983**, *11*, 1579−1588.
(30) Nishimura, Y.; Tsuboi, M.; Sato, T. *Nucleic Acids Res.* **1984**, *12*, 6901−6908.
(31) Peticolas, W. A.; Kubasek, W. L.; Thomas, G. A.; Tsuboi, M. *Nucleic Acids*; Peticolas, W. A., Kubasek, W. L., Thomas, G. A., Tsuboi, M., Eds.; John Wiley and Sons: New York, 1987; Vol. 1, pp 82−133.
(32) Ziegler, L. D.; Hudson, B.; Strommen, D. P.; Peticolas, W. L. *Biopolymers* **1984**, *23*, 2067−2081.
(33) Tsuboi, M.; Nishimura, Y.; Hirakawa, A. Y.; Peticolas, W. L. *Resonance Raman spectroscopy and normal modes of the nucleic acid bases*; Tsuboi, M., Nishimura, Y., Hirakawa, A. Y., Peticolas, W. L., Eds.; John Wiley and Sons: New York, 1988; Vol. 2, pp 109−179.
(34) Toyama, A.; Takino, Y.; Takeuchi, H.; Harada, I. *J. Am. Chem. Soc.* **1993**, *115*, 11092−11098.
(35) Toyama, A.; Kurashiki, E.; Watanabe, Y.; Takeuchi, H.; Harada, I. *J. Am. Chem. Soc.* **1991**, *113*, 3615−3616.
(36) Fodor, S. P. A.; Rava, R. P.; Hays, T. R.; Spiro, T. G. *J. Am. Chem. Soc.* **1985**, *107*, 1520−1529.
(37) Pohl, F. M.; Ranade, A.; Stockburger, M. *Biochim. Biophys. Acta* **1973**, *335*, 85−92.

10.1021/la025613z CCC: $22.00
Published on Web 05/04/2002

tional spectra and energetics of the individual nucleic acids and the AT and GC base pairs have also been studied by semiempirical and density functional theory (DFT) calculations.[47−49]

Self-assembled monolayers (SAMs) of DNA are prepared as mixed monolayers from a co-deposition solution of 6-mercapto-1-hexanol and single-stranded DNA (ssDNA) followed by surface hybridization with the complementary ssDNA.[50] Here we report the first direct detection of DNA hybridization on a gold surface using polarization modulation infrared reflection absorption spectroscopy (PM-IRRAS). The advantages of PM-IRRAS are threefold. First, labeling of the DNA with fluorescent tags or radioisotopes is not required. This technique is also nonintrusive allowing quick determination of the presence of single-stranded DNA or double-stranded DNA (dsDNA) on the surface without contaminating the sample with an electrochemical agent. Third, this technique can distinguish between the A, B, and Z forms of dsDNA on the surface. Single-pass attenuated total reflection (ATR)-FTIR spectra were taken of the ssDNA and dsDNA samples to verify the modes obtained with PM-IRRAS. ATR-FTIR spectra were also taken at various levels of hydration to determine the degree of hydration of the DNA strands on the surface. These comparisons provide an experimental link between bulk samples and analytical applications for detecting 10 pmol (based on the surface coverage of DNA and the sampling area of PM-IRRAS) of DNA or less on a surface.[10] The experiments performed here establish the application of grazing angle FTIR spectroscopy to the observation of DNA hybridization and detection of DNA−drug interactions using surface-attached DNA. DFT calculations of the individual DNA bases and base pairs were performed to yield calculated frequency spectra of ssDNA and dsDNA that were in excellent agreement with experimentally observed bands.

Methods and Materials

DNA Monolayer Formation. The mixed SAMs were prepared on clean polycrystalline gold deposited on a glass slide containing a chromium oxide passivation layer (Evaporated Films, Inc., cleaned with piranha solution (70% concentrated H_2SO_4/30% H_2O_2 (30%)) (CAUTION: piranha solution reacts violently with organic chemicals) and rinsed with Millipore 18 MΩ deionized water (Barnstead E-PURE). The ssDNA (Applied Biosystems) probe strand was modified at the 5′ end with a C6−S−disulfide modifier (Applied Biosystems). The ssDNA was deprotected to form the C6−SH linker as described elsewhere.[10] A co-deposition solution of 6-mercapto-1-hexanol (MCH) (Sigma-Aldrich) and ssDNA (probe strand) was used to form the mixed SAM on the gold surface with a 0.10 mole fraction of ssDNA in a 1 μM MCH solution in 1 M potassium phosphate buffer (pH 7.0) for 16 h at room temperature. The gold slides were then rinsed with 18 MΩ cm water and placed in a 1X SSC (saline sodium citrate) (Fisher Scientific) at 65 °C for 1 h and then cooled to room temperature over 4 additional hours with or without target ssDNA (exact complement to the probe ssDNA on the gold surface) for hybridization (2.5 nmol of target ssDNA). The surfaces were then rinsed in 18 MΩ cm water and dried with nitrogen gas. Both ssDNA strands were comprised of 30 bases; the probe strand had a sequence of 5′-GGAGACTGTTATCCGCTCA-CAATTCCACAC-3′, and the target ssDNA was the exact complement of the probe ssDNA strand. The solution hybridization mixture, containing the two complementary ssDNA strands (in 1X SSC), was heated to 85 °C for 5 min and then cooled to room temperature for 30 min to obtain dsDNA for solution FTIR measurements. The excess salt from the dsDNA solution was removed using Centricon YM-3 centrifugal filter units (Millipore) and 18 MΩ cm water as the wash solvent.

Polarization Modulation Infrared Reflection Absorption Spectroscopy. The PM-IRRAS spectra were recorded on a Digilab FTS 7000 (Randolph, MA) spectrometer equipped with a step scan interferometer, a liquid nitrogen cooled narrow band MCT detector, a globar source, and a UDR-8 filter. The IR radiation was typically phase modulated at frequencies of 400 or 800 Hz at an amplitude of 1.0 or 2.0 λ HeNe while stepping at 0.5−2.5 Hz. A gold grid polarizer was used to obtain either s- or p-polarized radiation, which was then modulated by a Hinds ZnSe PEM operating at 37 kHz and an amplitude of 0.5 λ (strain axis 45° to the polarizer) before reflecting off the sample at an incident angle of 80° from the surface normal. The spectra were recorded at room temperature at a resolution of 8 cm^{-1} and were the result of four scans with a spectral range of 900−1800 cm^{-1}. The digital signal processing (DSP) algorithm incorporated into the Bio-Rad spectrometer software was used to obtain the spectra. This instrument allowed the gold slide containing the monolayer to also be the reference to obtain the absorption spectra. The solution single-pass ATR-FTIR spectra of the DNA (∼20−200 mM) were taken using an IR microscope (model number UMA-500) attached to a Bio-Rad (now Digilab) FTS 6000 FTIR spectrometer equipped with a Cassegranian objective containing a germanium crystal for single-pass ATR. The spectrometer was equipped with a liquid nitrogen cooled MCT/A detector, and the spectra were recorded at a resolution of 2 cm^{-1} with a spectral range of 650−4000 cm^{-1}. The absorption spectra were the result of the average of multiples of 64 scans and were recorded at room temperature.

Density Functional Theory Calculations. The geometry optimization and vibrational frequency calculations of the individual DNA bases and complementary base pairs were done using the MSI (Molecular Simulations, Inc.) quantum chemistry software program DMol3 at the North Carolina Supercomputer Center (NCSC) on the IBM RS/6000 SP. DMol3 is an ab initio (first principles) software package that utilizes density functional theory.[51] These calculations were done in the gas phase using the DNP basis set, the GGA functional, and the method of finite differences for calculating the vibrational frequencies. The MSI software Insight II was used to build the models and to visualize the eigenvector projections of the vibrational modes of the models.

Results and Discussion

Parts A and B of Figure 1 show the PM-IRRAS spectra corresponding to the mixed monolayer of MCH and ssDNA before and after hybridization with the complementary ssDNA with a hybridization temperature of 65 and 85 °C, respectively, recorded at an incident angle of 80°. The hybridization temperature was varied to obtain efficient hybridization while minimizing ssDNA strand loss from the gold surface. The ssDNA and dsDNA spectra contain absorptive features indicative of DNA for both temperatures. For instance, the modes centered at 1082 and 1238 cm^{-1} correspond to the symmetric and asymmetric PO_2^-

(38) Erfurth, S. C.; Kiser, E. J.; Peticolas, W. L. *Proc. Natl. Acad. Sci. U.S.A.* **1972**, *69*, 938−941.
(39) Erfurth, S. C.; Bond, P. J.; Peticolas, W. L. *Biopolymers* **1975**, *14*, 1245−1257.
(40) Benevides, J. M.; Thomas, G. J., Jr. *Nucleic Acids Res.* **1983**, *11*, 5747−5761.
(41) LaFleur, L.; Rice, J.; Thomas, G. J., Jr. *Biopolymers* **1972**, *11*, 2423−2437.
(42) Thamann, T. J.; Lord, R. C.; Wang, A. H. J.; Rich, A. *Nucleic Acids Res.* **1981**, *9*, 5443−5457.
(43) Lu, D. S.; Nonaka, Y.; Tsuboi, M.; Nakamoto, K. *J. Raman Spectrosc.* **1990**, *21*, 321−326.
(44) Takeuchi, H.; Sasamori, J. *Biopolymers* **1995**, *35*, 359−367.
(45) Hud, N. V.; Milanovich, F. P.; Balhorn, R. *Biochemistry* **1994**, *33*, 7528−7535.
(46) Grygon, C. A.; Spiro, T. G. *Biochemistry* **1989**, *28*, 4397−4402.
(47) Hrouda, V.; Florian, J.; Hobza, P. *J. Phys. Chem.* **1993**, *97*, 1542−1557.
(48) Florian, J.; Leszczynski, J.; Johnson, B. G. *J. Mol. Struct.* **1995**, *349*, 421−426.
(49) Guerra, C.; Bickelhaupt, F.; Snijders, J.; Baerends, E. *J. Am. Chem. Soc.* **2000**, *122*, 4117−4128.
(50) Herne, T. M.; Tarlov, M. J. *J. Am. Chem. Soc.* **1997**, *119*, 8916−8920.
(51) Delley, B. *J. Phys. Chem.* **1990**, *92*, 508−517.

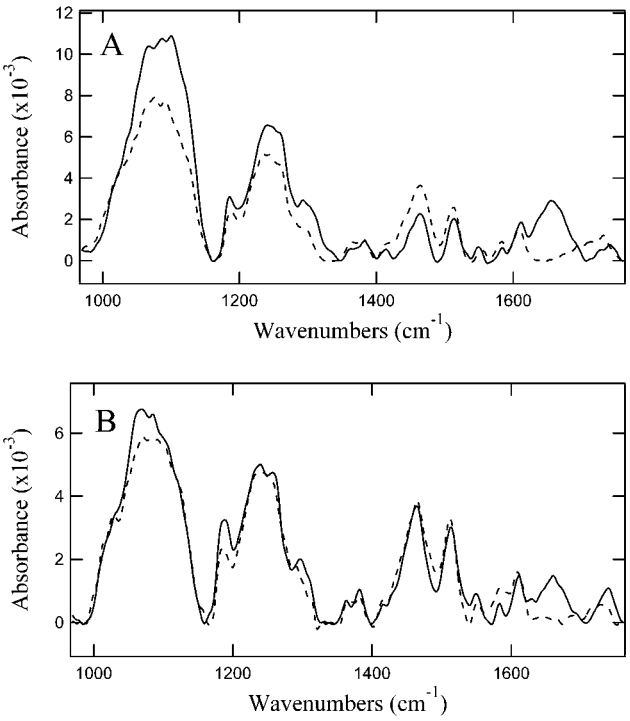

Figure 1. PM-IRRAS spectra of a mixed monolayer of 6-mercapto-1-hexanol and single-stranded DNA before (dashed spectrum) and after hybridization (solid spectrum) with the complementary single-stranded DNA strand to obtain double-stranded DNA with a hybridization temperature of 65 °C (A) or 85 °C (B) recorded at an incident angle of 80°.

group of the DNA phosphodiester backbone.[52,53] The mode centered at 1188 cm^{-1} is a well-known deoxyribose structural marker mode.[54] The combination of the asymmetric PO_2^- group mode at 1238 cm^{-1} and the deoxyribose mode at 1188 cm^{-1} is indicative of A-form DNA structure consistent with the low-humidity environment in the current PM-IRRAS configuration.[54,55] The modes at 1464 and 1514 cm^{-1} result from the purine and pyrimidine (DNA bases) ring modes,[52,53] while the region from 1600 to 1750 cm^{-1} is due to carbonyl (C═O), C═N stretching, and exocyclic $-NH_2$ bending vibrations in the DNA bases.[52,56] However, the intensities of these bands are not the same at 65 and 85 °C due to the quantity and orientation of the DNA on the surface. The intensity for the ssDNA and dsDNA spectra for 85 °C is lower than that of the corresponding spectra with a hybridization temperature of 65 °C. This observation suggests that strand loss is occurring at the higher temperature due to thiolate desorption.

The major distinction between the PM-IRRAS spectra for ssDNA and dsDNA in parts A and B of Figure 1 is the presence of a band at 1655 cm^{-1} in the dsDNA spectra, which is absent in the ssDNA spectra. This distinction is observed at both hybridization temperatures. The intensity change in this region represents changes in hydrogen bonding between complementary bases that occur upon formation of a double helix and the quantity of DNA on the surface.[52] The infrared signature at 1655 cm^{-1} of

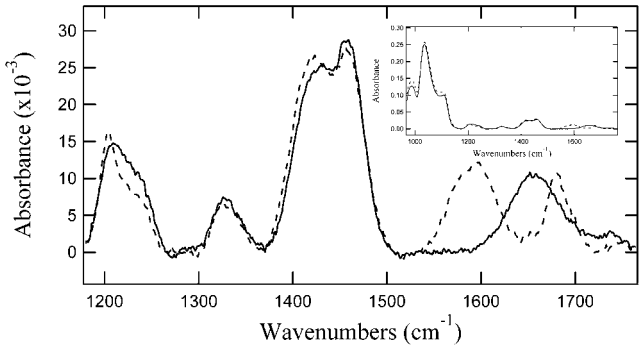

Figure 2. Solution single-pass ATR-FTIR spectra of single-stranded DNA (dashed spectrum) and double-stranded DNA (solid spectrum) corresponding to the same DNA strands used for the probe and target single-stranded DNA on the gold surfaces. The concentration of the DNA solutions was approximately 200 mM. The inset shows the larger spectral range from 970 to 1760 cm^{-1}.

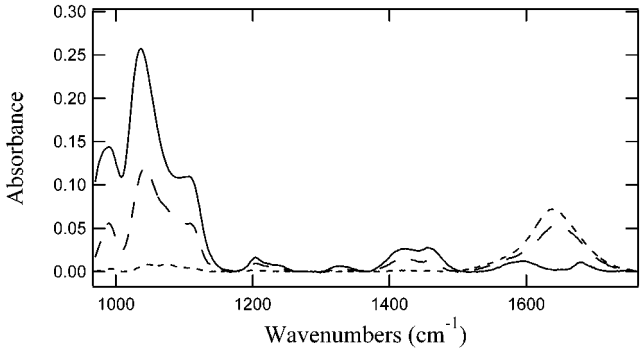

Figure 3. Solution single-pass ATR-FTIR spectra of single-stranded DNA recorded as a function of hydration and concentration in aqueous solution. The spectra correspond to least concentrated (∼20 mM) (short-dashed spectrum), more concentrated (long-dashed spectrum), and most concentrated (∼200 mM) (solid spectrum) samples of the single-stranded DNA used as the probe strand on the gold surfaces. The most concentrated sample is nearly in a gel state.

dsDNA thus permits the detection of DNA hybridization on gold surfaces by PM-IRRAS.

Figure 2 shows the single-pass ATR-FTIR spectra of ssDNA and dsDNA strands in aqueous solution to verify that the absorptive features observed in the PM-IRRAS spectra of ssDNA and dsDNA are due to these DNA species. These spectra contain similar features as seen in the PM-IRRAS spectra corresponding to these species on a gold surface. However, the absorptive features present in Figure 2 for ssDNA and dsDNA are not identical due to the hydrogen bonding between complementary bases in the dsDNA.[52] The features can be assigned, as done above, to arising from the phosphodiester backbone and the purine and pyrimidine rings of the DNA bases. However, ssDNA has two modes in the high-frequency region at 1594 and 1681 cm^{-1} that are replaced with a single mode at 1658 cm^{-1} in dsDNA. Therefore, ssDNA and dsDNA can be distinguished both in solution and on the gold surface using infrared spectroscopy. The sample conditions under single-pass ATR-FTIR resemble those of a hydrated DNA fiber.[54]

Figure 3 shows the single-pass ATR-FTIR spectra of ssDNA in aqueous solution as a function of hydration to estimate the amount of hydration in the DNA monolayers on the gold surfaces. Initially, the bending vibration mode of water at 1638 cm^{-1} masks the carbonyl and amino hydrogen-bonding region of the spectra and the other modes in the spectra cannot be discerned due to a low

(52) Tsuboi, M. *Prog. Theor. Phys. Suppl.* **1961**, *17*, 99−107.
(53) Falk, M.; Hartman, K. A.; Lord, R. C. *J. Am. Chem. Soc.* **1963**, *85*, 391−394.
(54) Taillandier, E.; Liquier, J. *Methods Enzymol.* **1992**, *211*, 307−335.
(55) Taillandier, E.; Liquier, J.; Ghomi, M. *J. Mol. Struct.* **1989**, *214*, 185−211.
(56) Liquier, J.; Coffinier, P.; Firon, M.; Taillandier, E. *J. Biomol. Struct. Dyn.* **1991**, *9*, 437−445.

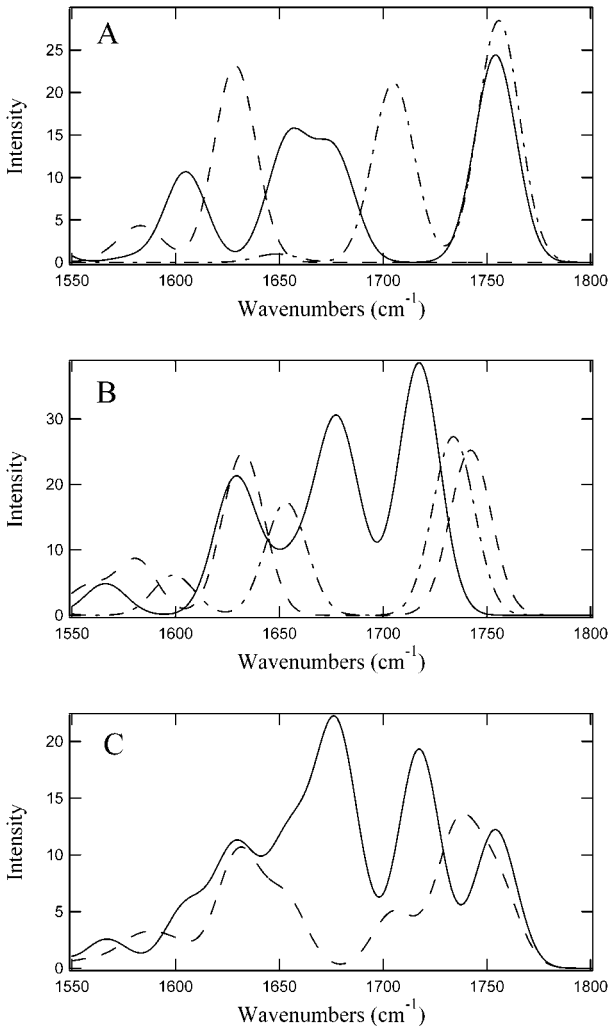

Figure 4. Calculated infrared spectra of (A) adenine (dashed spectrum), thymine (dashed−dotted spectrum), and the adenine−thymine base pair (solid spectrum); (B) guanine (dashed spectrum), cytosine (dashed−dotted spectrum), and the guanine−cytosine base pair (solid spectrum); (C) probe ssDNA before (dashed spectrum) and after hybridization (dsDNA) (solid spectrum) using the weighted average of the calculated spectra of either the individual bases or base pairs, respectively. All spectra have a Gaussian width of 10 cm^{-1}.

concentration of DNA.[17] However, as the water begins to evaporate the concentration of the DNA in the IR radiation path begins to increase and the masking bending mode of water begins to decrease. Finally, only water of hydration is present in the sample permitting observations of the absorptive features of the DNA. On the basis of the absence of the water bending mode in the PM-IRRAS spectra, it can be concluded that only the water of hydration is present on the gold surface of the DNA monolayers.

Figure 4 shows the DFT-calculated infrared spectra of the individual DNA bases, DNA base pairs, and their weighted average to obtain calculated infrared spectra corresponding to the ssDNA and dsDNA used in the DNA monolayers on gold. Figure 4A specifically shows the DFT-calculated vibrational spectrum of adenine, thymine, and the adenine−thymine (AT) base pair in the 1550−1800 cm^{-1} region. The adenine calculated spectrum has three modes at 1572, 1584, and 1629 cm^{-1} due mostly from NH_2 bending (and some ring deformation). The thymine calculated spectrum has a mode at 1649 cm^{-1} due to C−C stretching and two modes at 1705 and 1756 cm^{-1} resulting from carbonyl stretching. The calculated spectrum of the AT base pair resulted in four modes at 1605, 1655, 1676, and 1754 cm^{-1}. The modes at 1605 and 1655 cm^{-1} result from NH_2 bending, the mode at 1642 cm^{-1} is a ring deformation mode, the mode at 1676 cm^{-1} results from N−H bending, and the mode at 1754 cm^{-1} results from a carbonyl stretching motion. These spectra illustrate a blue shift of the NH_2 bending modes upon base pair formation due to hydrogen bonding which involves this group. The NH_2 bending motion of adenine becomes more constrained in the base pair, and hence the frequency of the NH_2 bend increases. The carbonyl stretching frequency of the carbonyl group of thymine involved in hydrogen bonding in the AT base pair decreases in frequency upon base pair formation. This red shift is the result of a weakening of the C═O force constant due to hydrogen bonding. The other carbonyl stretching frequency of thymine decreases minimally since this carbonyl group is not involved in hydrogen bonding with adenine in the AT base pair. These shifts are in qualitative agreement with previous semiempirical calculations.[47]

Figure 4B shows the DFT-calculated infrared spectra of guanine, cytosine, and the guanine−cytosine (GC) base pair in the region of 1550−1800 cm^{-1}. The calculated spectrum of guanine shows two modes at 1582 and 1632 cm^{-1} primarily due to NH_2 bending and one carbonyl stretching mode at 1742 cm^{-1}. The cytosine calculated frequency spectrum shows two modes at 1524 and 1653 cm^{-1} resulting from ring deformation (and C═N stretching), a mode at 1599 cm^{-1} due to NH_2 bending, and a carbonyl stretching mode at 1733 cm^{-1}. The GC base pair calculated frequency spectrum shows six modes at 1565 cm^{-1} (NH_2 and N−H bending, carbonyl stretching), 1628 and 1634 cm^{-1} (primarily NH_2 and N−H bending, small component of carbonyl stretching and ring deformation), 1676 cm^{-1} (NH_2 bending, carbonyl stretching), and 1684 and 1717 cm^{-1} (NH_2 and N−H bending, carbonyl stretching). Similar to the calculated spectrum of the AT base pair relative to the spectra of the individual bases, the GC calculated spectrum shows a blue shift in the NH_2 (and N−H) bending frequency and a red shift in the carbonyl stretching frequency for those groups involved in hydrogen bonding in the GC base pair relative to the individual bases.

Figure 4C shows the DFT-calculated infrared spectra corresponding to the probe ssDNA strand and the dsDNA (after hybridization with target ssDNA) strand used in the monolayers on gold in the 1550−1800 cm^{-1} region. These spectra were obtained by weighting the individual (for ssDNA) or the base pair (for dsDNA) spectra in the appropriate amount corresponding to the sequence of the probe and target ssDNA strands used. These show the NH_2 and N−H bending modes and the carbonyl stretching frequencies as discussed above for the individual bases and base pairs. The main difference between these two spectra is the existence of an infrared signature mode at 1676 cm^{-1} in the dsDNA spectrum that is absent in the calculated ssDNA spectrum. This result is consistent with the observed differences in the surface and bulk FTIR spectra of the corresponding ssDNA and dsDNA strands. The models and the eigenvector projections of these modes are in the Supporting Information.

Conclusion

Polarization modulation infrared reflection absorption spectroscopy (PM-IRRAS) was successfully used to detect DNA hybridization on a gold surface. The most pronounced spectral changes between ssDNA and dsDNA are in the

nucleobase hydrogen-bonding region from 1550 to 1720 cm^{-1}. Surface hybridization was detected by an increase in absorption intensity at 1655 cm^{-1} in dsDNA. Comparison of the single-pass ATR-FTIR spectra of ssDNA solutions with the PM-IRRAS method showed that a minimal amount of water was present in the DNA monolayers on gold due to the absence of the water bending mode, ν_{H-O-H}, at 1638 cm^{-1} in the PM-IRRAS spectra. This observation is significant because, if present, ν_{H-O-H} masks the region of the DNA spectrum that contains the most information. The spectral features of surface-attached DNA are similar to those of fiber DNA at low humidity.[54] However, ssDNA does not form fibers, and thus the conversion of ssDNA to dsDNA cannot be detected by FTIR spectroscopy so that the observed spectral changes associated with hybridization reported here are unique. The PM-IRRAS spectra were in excellent agreement with DFT-calculated spectra of dsDNA and ssDNA. The calculated infrared spectra of the DNA bases and base pairs show that the difference between ssDNA and dsDNA results from the blue shift of the NH_2 and N−H bending modes and a red shift in the carbonyl stretching frequency due to hydrogen bonding between the complementary bases. These changes permit detection of DNA hybridization on samples for which the surface coverage is 4×10^{12} molecules/cm^2.[10] The measurements shown in Figure 1 demonstrate the feasibility of detecting DNA hybridization on samples with this surface coverage. These results suggest that the PM-IRRAS technique can be used to observe binding events to surface-immobilized DNA. The fact that A-form structure is observed in the spectra presented here indicates that the current configuration can be used directly to observe binding events to surface-immobilized RNA. The PM-IRRAS method can be used in theory in high-humidity conditions favoring B-form DNA. Thus, in addition to the detection of DNA hybridization, PM-IRRAS has the potential for use in the study of protein and drug binding to RNA and DNA.

Acknowledgment. Scott Brewer was supported by NIH Biotechnology Training Grant T32-GM08776. Support and computational facilities were provided by the North Carolina Supercomputing Center.

Supporting Information Available: Models and eigenvector projections for the vibrational modes of the DNA bases. This material is available free of charge via the Internet at http://pubs.acs.org.

LA025613Z